

Contents lists available at ScienceDirect

Applied Mathematics Letters

www.elsevier.com/locate/aml



A linear energy and entropy-production-rate preserving scheme for thermodynamically consistent crystal growth models*,***



Yucan Zhao a, Jun Li c, Jia Zhao d, Qi Wang b,a,*

- ^a Beijing Computational Science Research Center, Beijing 100193, PR China
- ^b Department of Mathematics, University of South Carolina, Columbia, SC 29028, USA
- ^c School of Mathematical Sciences, Tianjin Normal University, Tianjin 300387, PR China
- ^d Department of Mathematics and Statistics, Utah State University, Logan, UT 84322, USA

ARTICLE INFO

Article history: Received 12 April 2019 Received in revised form 19 May 2019 Accepted 19 May 2019 Available online 5 June 2019

Keywords:
Thermodynamically consistent phase field model
Energy and entropy-production-rate preserving scheme
Energy quadratization (EQ)
Scalar auxiliary variable (SAV)
Crystal growth

ABSTRACT

We present a linear, second order, energy and entropy-production-rate preserving scheme for a thermodynamically consistent phase field model for dentritic crystal growth, combining an energy quadratization strategy with the finite element method. The scheme can be decomposed into a series of Poisson equations for efficient numerical implementations. Numerical tests are carried out to verify the accuracy of the scheme and simulations are conducted to demonstrate the effectiveness of the scheme on benchmark examples.

© 2019 Elsevier Ltd. All rights reserved.

1. Introduction

The Penrose–Fife model has been used to describe dentritic crystal growth in a binary mixture [1]. This model is thermodynamically consistent in that the internal energy is conserved while the total entropy of the system increases in time. Several numerical approximations have been proposed to solve the model, in particular, a linear, finite difference approximation based on the energy quadratization strategy has been recently proposed to solve it, which preserves the internal energy and the entropy-production-rate [2]. We refer readers for more references on this topic to [2]. In this letter, we present a complementary approach to devise a linear, second order, energy and entropy-production-rate preserving scheme for this model,

^{☆☆} The research is partially supported by NSF awards DMS-1517347, DMS-1815921, DMS-1816783, OIA-1655740 and a GEAR award from SC EPSCoR/IDeA Program, NSFC awards 11571032, 91630207, 11301287 and NSAF-U1530401, Tianjin Normal University Foundation for the introduction of talent (5RL154).

^{*} Corresponding author at: Department of Mathematics, University of South Carolina, Columbia, SC 29028, USA. E-mail addresses: zhaoyc@csrc.ac.cn (Y. Zhao), nkjunli@tjnu.edu.cn (J. Li), jia.zhao@usu.edu (J. Zhao), qwang@math.sc.edu (Q. Wang).

exploiting its thermodynamical consistency. Specifically, we employ two auxiliary scalar variables (SAV) to quadratize the total entropy into a quadratic form, from which we devise a linear, entropy-production-rate preserving scheme. The scheme can be effectively decomposed into a series of Poisson equations, amenable to fast solvers, making it a potentially efficient scheme. This letter outlines the scheme and its hierarchical solution procedures, and proves the entropy-production-rate preserving property as well as solvability of the linear system.

2. Thermodynamically consistent phase-field models for dendritic crystal growth and its SAV reformulation

The version of the thermodynamically consistent phase field model for dentritic crystal growth was derived and studied in [2]. In this model, a phase field variable ϕ is used to denote the material phase: $\phi=1$ denotes the solid phase and $\phi=0$ the liquid one. We denote the bulk internal energy by e, the bulk entropy by s, and the conformational entropy by s_1 , respectively. The total entropy is given by $S=\int_{\Omega}[s_1(\nabla\phi)+s(\phi,e)]d\mathbf{r}$, where Ω is the material domain, $s_1=-\frac{1}{2}\left|\kappa\left(\theta\right)\nabla\phi\right|^2$, κ is the anisotropy of the conformational entropy given by $\kappa=1+\epsilon_4 cos\left(m\left(\theta-\theta_0\right)\right)$ in 2D, m is the number of folds in space, and ϵ_4 is a parameter for the strength of anisotropy and θ_0 is a constant rotation angle. We assume there is no entropic flux across the material domain so that $\mathbf{n} \cdot B_s=0$, where $B_s=\frac{\partial s_1}{\partial \nabla \phi}\phi_t-\frac{\partial s}{\partial e}\mathbf{q}$ is the entropic flux, \mathbf{q} is the flux of the internal energy, and \mathbf{n} is the unit external normal to the boundary of Ω .

The governing system of equations in the model is given by

$$\tau \phi_{t} = \frac{\delta S}{\delta \phi} = Q(T) p'(\phi) - F'(\phi) + \epsilon^{2} \nabla \cdot \left(\kappa \left| \nabla \phi \right|^{2} \frac{\partial \kappa}{\partial \nabla \phi} + \kappa^{2} \nabla \phi \right),$$

$$e_{t} = -\nabla \cdot \left(D_{u} T^{2} \nabla \frac{\delta S}{\delta e} \right).$$
(1)

where T is the absolute temperature, $D_u > 0$ is the heat conductivity and $\tau = \tau(\theta(\phi)) > 0$ is the relaxation time coefficient.

For the thermodynamically consistent model, we aim to develop a linear, structure-preserving approximation using the SAV entropy quadratization technique [3]. We introduce two scalar auxiliary variables for this purpose

$$U = \sqrt{\int_{\Omega} \left(\epsilon^2 \left(\kappa^2 - k_0 \right) \left| \nabla \phi \right|^2 + 2B \right) d\mathbf{r}}, q = \sqrt{\int_{\Omega} \left(2 \left(-s - \frac{C_0}{2} \phi^2 - \frac{C_1}{2} e^2 + A \right) \right) d\mathbf{r}}. \tag{2}$$

Using the new variables, we transform the total entropy into a quadratic form

$$S = \int_{\Omega} \left(-\frac{\epsilon^2 k_0}{2} \left| \nabla \phi \right|^2 - \frac{C_0}{2} \phi^2 - \frac{C_1}{2} e^2 + A + B \right) d\mathbf{r} - \frac{1}{2} U^2 - \frac{1}{2} q^2, \tag{3}$$

where C_0, C_1, A, B are user-specified constants to ensure U and q are real-valued. The variational derivatives are given by

$$\frac{\delta S}{\delta \phi} = \epsilon^2 k_0 \Delta \phi - C_0 \phi + \nabla \cdot [U\mathbf{H}] - qg, \frac{\delta S}{\delta e} = -C_1 e - qh. \tag{4}$$

Let T_M be critical temperature, $e_L(T)$ the internal energy at the liquid phase, L_0, L_1 parameters in the energy, and C_L the specific heat for the liquid phase. Then,

$$g(\phi, e) = \frac{\partial q}{\partial \phi}, h(\phi, e) = \frac{\partial q}{\partial e}, L_{U} = \epsilon^{2} \left(\kappa^{2} - k_{0}\right) \left|\nabla\phi\right|^{2} + 2B, \mathbf{H}\left(\nabla\phi\right) = \frac{1}{2U} \frac{\partial L_{U}}{\partial \nabla\phi},$$

$$\kappa = 1 + \epsilon_{4} cos\left(m\left(\theta - \theta_{0}\right)\right),$$

$$s(\phi, e) = \frac{e}{T} + \int_{T_{M}}^{T} \frac{e_{L}(\xi)}{\xi^{2}} d\xi + \left(p\left(\phi\right) - 1\right) Q\left(T\right) - F\left(\phi\right), F\left(\phi\right) = \frac{1}{4}\phi^{2} \left(1 - \phi\right)^{2}, De\left(\phi, e\right) = DuT^{2},$$

$$T\left(\phi, e\right) = \frac{1}{C_{L} + (p(\phi) - 1)L_{1}} \left[e - e_{L}(T_{M}) + C_{L}T_{M} - \left(p\left(\phi\right) - 1\right)(L_{0} - L_{1}T_{M})\right],$$

$$p(\phi) = 30 \left(\frac{1}{5}\phi^{5} - \frac{1}{2}\phi^{4} + \frac{1}{3}\phi^{3}\right),$$

$$Q\left(T\right) = \left(L_{0} - L_{1}T_{M}\right) \left(\frac{1}{T} - \frac{1}{T_{M}}\right) + \left(L_{1}\right) \left(lnT - lnT_{M}\right), e = e_{L}\left(T_{M}\right) + C_{L}\left(T - T_{M}\right) + \left(p\left(\phi\right) - 1\right)\left(L_{0} + L_{1}\left(T - T_{M}\right)\right).$$

$$(5)$$

We add time derivatives of U and q to (1) to arrive at the reformulated equation system of the model

$$\tau \phi_{t} = \frac{\delta S}{\delta \phi} = \left(\epsilon^{2} k_{0} \Delta \phi - C_{0} \phi + U \nabla \cdot [\mathbf{H}] - qg \right),
e_{t} = -\nabla \cdot \left(D_{e} \nabla \left(\frac{\delta S}{\delta e} \right) \right) = -\nabla \cdot \left(D_{e} \nabla \left(-C_{1} e - qh \right) \right),
U_{t} = \int_{\Omega} \mathbf{H} \cdot (\nabla \phi)_{t} d\mathbf{r}, \quad q_{t} = \int_{\Omega} \left(g \phi_{t} + h e_{t} \right) d\mathbf{r},$$
(6)

where $\mathbf{H} = \frac{\partial U}{\partial \nabla \phi}$. These equations will be supplied with initial conditions: $\phi(x,y,t=0) = \phi_0(x,y)$, $e(x,y,t=0) = e_0(x,y)$, where ϕ_0 and e_0 are prescribed functions, and physical boundary conditions: $\mathbf{n} \cdot (U\mathbf{H} + \epsilon^2 k_0 \nabla \phi) = 0$ and $\mathbf{n} \cdot \nabla (C_1 e + qh) = 0$ or periodic boundary conditions. In this letter, we present our results for periodic boundary conditions for simplicity. For the Neumann physical boundary conditions, the result is valid as well. If the boundary condition induces entropy changes, the boundary effect will have to be accounted for in entropy production, which is a new problem. We note that this model conserves the internal energy and has a positive entropy production rate

$$\frac{d}{dt} \int_{\Omega} e d\mathbf{r} = 0, \frac{dS}{dt} = \int_{\Omega} \left(\tau(\phi_t)^2 - \frac{\delta S}{\delta e} e_t \right) d\mathbf{r} = \int_{\Omega} \left(\tau(\phi_t)^2 + \nabla (C_1 e + qh) \cdot De \nabla (C_1 e + qh) \right) d\mathbf{r} \ge 0. \quad (7)$$

3. Numerical algorithms—energy stability and solvability

We now proceed to develop an efficient, linear, structure-preserving scheme for (6). We first present a semi-discrete scheme in time and then discuss its spatial discretization using a finite element method later.

Scheme 1 (Semidiscrete Energy Stable Scheme). After obtaining $(\phi^n, e^n), (\phi^{n-1}, e^{n-1})$, we compute (ϕ^{n+1}, e^{n+1}) using the following scheme:

$$\bar{\tau}^{n+1/2}\delta_{t}(\phi)^{n} = \frac{\delta S}{\delta \bar{\phi}}^{n+1/2} = \epsilon^{2}k_{0}\Delta\phi^{n+1/2} - C_{0}\phi^{n+1/2} + \nabla \cdot \left[U^{n+1/2}\bar{\mathbf{H}}^{n+1/2}\right] - q^{n+1/2}\bar{g}^{n+1/2},$$

$$\delta_{t}(e)^{n} = -\nabla \cdot \left[\bar{D}e^{n+1/2}\nabla\left(\frac{\delta S}{\delta e}^{n+1/2}\right)\right] = -\nabla \cdot \left(\bar{D}e^{n+1/2}\nabla\left(-C_{1}e^{n+1/2} - q^{n+1/2}\bar{h}^{n+1/2}\right)\right),$$

$$\delta_{t}(U)^{n} = \int_{\Omega}\bar{\mathbf{H}}^{n+1/2} \cdot \delta_{t}(\nabla\phi)^{n}d\mathbf{r}, \quad \delta_{t}(q)^{n} = \int_{\Omega}\left(\bar{g}^{n+1/2}\delta_{t}(\phi)^{n} + \bar{h}^{n+1/2}\delta_{t}(e)^{n}\right)d\mathbf{r},$$
(8)

where
$$\delta_t(\bullet)^n = \frac{(\bullet)^{n+1} - (\bullet)^n}{\Delta t}$$
, $(\bullet)^{n+1/2} = \frac{1}{2} \left((\bullet)^{n+1} + (\bullet)^n \right)$, $(\stackrel{-}{\bullet})^{n+1/2} = \frac{1}{2} \left(3 (\bullet)^n - (\bullet)^{n-1} \right)$.

We rewrite the first two equations in (8) by eliminating U^{n+1} and q^{n+1} as follows,

$$A_{1}\phi^{n+1} + d_{1}^{n} \langle \bar{\mathbf{H}}^{n+1/2}, \nabla \phi^{n+1} \rangle + d_{2}^{n} [\langle \bar{g}^{n+1/2}, \phi^{n+1} \rangle + \langle \bar{h}^{n+1/2}, e^{n+1} \rangle] = b_{1}^{n},$$

$$A_{2}e^{n+1} + d_{3}^{n} [\langle \bar{g}^{n+1/2}, \phi^{n+1} \rangle + \langle \bar{h}^{n+1/2}, e^{n+1} \rangle] = b_{2}^{n},$$

$$(9)$$

where $A_1 = \mathbf{I} - \frac{\Delta t}{2} \frac{1}{\bar{\tau}^{n+1/2}} \epsilon^2 k_0 \Delta + \frac{\Delta t}{2} \frac{1}{\bar{\tau}^{n+1/2}} C_0$, $A_2 = \mathbf{I} - \frac{\Delta t}{2} C_1 \nabla \cdot (\bar{D_e}^{n+1/2} \nabla)$, $b_1^n = \phi^n + \frac{\Delta t}{2} \frac{1}{\bar{\tau}^{n+1/2}} \epsilon^2 k_0 \Delta \phi^n - \frac{\Delta t}{2} \frac{1}{\bar{\tau}^{n+1/2}} C_0 \phi^n + \frac{1}{\bar{\tau}^{n+1/2}} \Delta t U^n \nabla \cdot \left[\bar{\mathbf{H}}^{n+1/2}\right] - \frac{\Delta t}{2} \frac{1}{\bar{\tau}^{n+1/2}} \nabla \cdot \left[\bar{\mathbf{H}}^{n+1/2}\right] \left\langle \bar{\mathbf{H}}^{n+1/2}, \nabla \phi^n \right\rangle - \frac{1}{\bar{\tau}^{n+1/2}} \Delta t q^n \bar{g}^{n+1/2} + \frac{\Delta t}{2} \frac{\bar{g}^{n+1/2}}{\bar{\tau}^{n+1/2}} \left[\left\langle \bar{g}^{n+1/2}, \phi^n \right\rangle + \left\langle \bar{h}^{n+1/2}, e^n \right\rangle \right], \ b_2^n = e^n + \frac{\Delta t}{2} C_1 \nabla \cdot \left(\bar{D_e}^{n+1/2} \nabla e^n \right) + \Delta t q^n \nabla \cdot \left(\bar{D_e}^{n+1/2} \nabla \bar{h}^{n+1/2} \right) - \frac{\Delta t}{2} \nabla \cdot \left(\bar{D_e}^{n+1/2} \nabla \bar{h}^{n+1/2} \right) \left[\left\langle \bar{g}^{n+1/2}, \phi^n \right\rangle + \left\langle \bar{h}^{n+1/2}, e^n \right\rangle \right], \ d_1^n = -\frac{\Delta t}{2} \frac{1}{\bar{\tau}^{n+1/2}} \nabla \cdot \left[\bar{\mathbf{H}}^{n+1/2}\right], \ d_2^n = \frac{\Delta t}{2} \frac{\bar{g}^{n+1/2}}{\bar{\tau}^{n+1/2}}, \ d_3^n = -\frac{\Delta t}{2} \nabla \cdot \left(\bar{D_e}^{n+1/2} \nabla \bar{h}^{n+1/2} \right), \ \langle u, v \rangle = \int_{\Omega} uv d\mathbf{r}, \ \langle \mathbf{a}, \mathbf{b} \rangle = \int_{\Omega} \mathbf{a} \cdot \mathbf{b} d\mathbf{r}. \ \text{Multiplying the two equations in (9)}$ by A_1^{-1} and A_2^{-1} and taking the inner product with $\nabla \cdot \bar{\mathbf{H}}^{n+1/2}, \ \bar{g}^{n+1/2}$ and $\bar{h}^{n+1/2}$ respectively, we obtain two equations

$$\begin{array}{l} (1+\left\langle \bar{\mathbf{H}}^{n+1/2},\nabla\left(A_{1}^{-1}d_{1}^{n}\right)\right\rangle)\left\langle \bar{\mathbf{H}}^{n+1/2},\nabla\phi^{n+1}\right\rangle + \left[\left\langle \bar{g}^{n+1/2},\phi^{n+1}\right\rangle + \left\langle \bar{h}^{n+1/2},e^{n+1}\right\rangle\right] \\ \left\langle \bar{\mathbf{H}}^{n+1/2},\nabla\left(A_{1}^{-1}d_{2}^{n}\right)\right\rangle = \left\langle \bar{\mathbf{H}}^{n+1/2},\nabla\left(A_{1}^{-1}b_{1}^{n}\right)\right\rangle, \\ (1+\left\langle \bar{g}^{n+1/2},A_{1}^{-1}d_{2}^{n}\right\rangle + \left\langle \bar{h}^{n+1/2},A_{2}^{-1}d_{3}^{n}\right\rangle)\left[\left\langle \bar{g}^{n+1/2},\phi^{n+1}\right\rangle + \left\langle \bar{h}^{n+1/2},e^{n+1}\right\rangle\right] + \\ \left\langle \bar{g}^{n+1/2},A_{1}^{-1}d_{1}^{n}\right\rangle\left\langle \bar{\mathbf{H}}^{n+1/2},\nabla\phi^{n+1}\right\rangle = \left\langle \bar{h}^{n+1/2},A_{2}^{-1}b_{2}^{n}\right\rangle + \left\langle \bar{g}^{n+1/2},A_{1}^{-1}b_{1}^{n}\right\rangle. \end{array} \tag{10}$$

The terms $A_1^{-1}d_1^n \doteq \eta_1^n$, $A_1^{-1}d_2^n \doteq \eta_2^n$, $A_1^{-1}b_1^n \doteq \eta_3^n$, $A_2^{-1}d_3^n \doteq \eta_4^n$ and $A_2^{-1}b_2^n \doteq \eta_5^n$ are evaluated by solving weak problems:

$$\langle A_{1}\eta_{1}^{n}, \xi_{1} \rangle = \langle d_{1}^{n}, \xi_{1} \rangle, \langle A_{1}\eta_{2}^{n}, \xi_{1} \rangle = \langle d_{2}^{n}, \xi_{1} \rangle, \langle A_{1}\eta_{3}^{n}, \xi_{1} \rangle = \langle b_{1}^{n}, \xi_{1} \rangle, \forall \xi_{1} \in H^{1}(\Omega),$$

$$\langle A_{2}\eta_{1}^{n}, \xi_{2} \rangle = \langle d_{3}^{n}, \xi_{2} \rangle, \langle A_{2}\eta_{5}^{n}, \xi_{2} \rangle = \langle b_{2}^{n}, \xi_{2} \rangle, \forall \xi_{2} \in H^{1}(\Omega).$$

$$(11)$$

Applying the Lax–Milgram theorem, we can easily establish that each equation in (11) admits a unique solution in $H^1(\Omega)$ with periodic boundary conditions.

Next, we discretize (9), (10) and (11) in space using the finite element method based on a conforming C^0 element [4,5]. We consider a triangulation \mathcal{T}_h over domain $\Omega = \bigcup_i T_i$, i.e. the set Ω is subdivided into a finite number of subsets T_i . We use a finite-dimensional space $V_h = \{u \in C(\overline{\Omega}) : u|_{T_i} = P_1(T_i), \forall T_i \in \mathcal{T}_h\}$ of piecewise polynomial functions u satisfying the periodic boundary conditions, where $P_k(T_i)$ are the restrictions of the polynomial functions to $T_i \in \mathcal{T}_h$ with degrees not higher than k. It is a finite dimensional subspace of the test and trial space in $H^1(\Omega)$ [6]. We present the fully discrete scheme below.

Scheme 2 (Fully Discrete Finite Scheme). The scheme consists of 7 hierarchical steps.

Step 1. Compute integrals $\left\langle \bar{\mathbf{H}}_{h}^{n+1/2}, \nabla \phi_{h}^{n} \right\rangle$ and $\left[\left\langle \bar{g}_{h}^{n+1/2}, \phi_{h}^{n} \right\rangle + \left\langle \bar{h}_{h}^{n+1/2}, e_{h}^{n} \right\rangle \right]$ using a composite formula consisting of Gaussian quadratures in elements.

Step 2. Evaluate the discrete functions: $(\eta_1^n)_h$, $(\eta_2^n)_h$, $(\eta_3^n)_h$, $(\eta_4^n)_h$ and $(\eta_5^n)_h \in V_h$ by solving:

$$\begin{split} \langle A_{1}\left(\eta_{1}^{n}\right)_{h},\left(\xi_{1}\right)_{h}\rangle &=\left\langle \left(d_{1}^{n}\right)_{h},\left(\xi_{1}\right)_{h}\right\rangle ,\left\langle A_{1}\left(\eta_{2}^{n}\right)_{h},\left(\xi_{1}\right)_{h}\right\rangle =\left\langle \left(d_{2}^{n}\right)_{h},\left(\xi_{1}\right)_{h}\right\rangle ,\\ \langle A_{1}\left(\eta_{3}^{n}\right)_{h},\left(\xi_{1}\right)_{h}\rangle &=\left\langle \left(b_{1}^{n}\right)_{h},\left(\xi_{1}\right)_{h}\right\rangle ,\left\langle A_{2}\left(\eta_{4}^{n}\right)_{h},\left(\xi_{2}\right)_{h}\right\rangle =\left\langle \left(d_{3}^{n}\right)_{h},\left(\xi_{2}\right)_{h}\right\rangle ,\\ \langle A_{2}\left(\eta_{5}^{n}\right)_{h},\left(\xi_{2}\right)_{h}\rangle &=\left\langle \left(b_{2}^{n}\right)_{h},\left(\xi_{2}\right)_{h}\right\rangle ,\forall\left(\xi_{1}\right)_{h},\forall\left(\xi_{2}\right)_{h}\in V_{h} \end{split}$$

 $\begin{array}{lll} \textbf{Step 3.} & \textit{Compute integrals} & \left\langle \bar{\mathbf{H}}_{h}^{n+1/2}, \nabla \left(\eta_{1}^{n} \right)_{h} \right\rangle, \\ \left\langle \bar{\mathbf{H}}_{h}^{n+1/2}, \nabla \left(\eta_{2}^{n} \right)_{h} \right\rangle, \\ \left\langle \bar{g}_{h}^{n+1/2}, \left(\eta_{3}^{n} \right)_{h} \right\rangle, \\ \left\langle \bar{g}_{h}^{n+1/2}, \left(\eta_{3}^{n} \right)_{h} \right\rangle, \\ \left\langle \bar{g}_{h}^{n+1/2}, \left(\eta_{3}^{n} \right)_{h} \right\rangle, \\ \left\langle \bar{h}_{h}^{n+1/2}, \left(\eta_{4}^{n} \right)_{h} \right\rangle, \\ \left\langle \bar{h}_{h}^{n+1/2}, \left(\eta_{5}^{n} \right)_{h} \right\rangle & \textit{using the composite formula consisting of Gaussian quadratures.} \end{array}$

Step 4. Solve
$$x_1 = \left\langle \bar{\mathbf{H}}_h^{n+1/2}, \nabla \phi_h^{n+1} \right\rangle$$
 and $x_2 = \left[\left\langle \bar{g}_h^{n+1/2}, \phi_h^{n+1} \right\rangle + \left\langle \bar{h}_h^{n+1/2}, e_h^{n+1} \right\rangle \right]$ from

$$\begin{bmatrix}
1 + \left\langle \bar{\mathbf{H}}_{h}^{n+1/2}, \nabla \left(\eta_{1}^{n}\right)_{h} \right\rangle & \left\langle \bar{\mathbf{H}}_{h}^{n+1/2}, \nabla \left(\eta_{2}^{n}\right)_{h} \right\rangle \\
\left\langle \bar{g}_{h}^{n+1/2}, \left(\eta_{1}^{n}\right)_{h} \right\rangle & 1 + \left\langle \bar{g}_{h}^{n+1/2}, \left(\eta_{2}^{n}\right)_{h} \right\rangle + \left\langle \bar{h}_{h}^{n+1/2}, \left(\eta_{4}^{n}\right)_{h} \right\rangle
\end{bmatrix} \cdot \begin{bmatrix} x_{1} \\ x_{2} \end{bmatrix} \\
= \begin{bmatrix} \left\langle \bar{\mathbf{H}}_{h}^{n+1/2}, \nabla \left(\eta_{3}^{n}\right)_{h} \right\rangle \\
\left\langle \bar{g}_{h}^{n+1/2}, \left(\eta_{3}^{n}\right)_{h} \right\rangle + \left\langle \bar{h}_{h}^{n+1/2}, \left(\eta_{5}^{n}\right)_{h} \right\rangle
\end{bmatrix} (13)$$

Step 5. Obtain ϕ_h^{n+1} and e_h^{n+1} by solving:

$$\left\langle A_{1}\phi_{h}^{n+1}, (\psi_{1})_{h} \right\rangle = \left\langle \left(\widetilde{b}_{1}^{n} \right)_{h}, (\psi_{1})_{h} \right\rangle, \forall (\psi_{1})_{h} \in V_{h},
\left\langle A_{2}e_{h}^{n+1}, (\psi_{2})_{h} \right\rangle = \left\langle \left(\widetilde{b}_{2}^{n} \right)_{h}, (\psi_{2})_{h} \right\rangle, \forall (\psi_{2})_{h} \in V_{h},$$
(14)

$$\begin{aligned} & where \, \left(\tilde{b}_{1}^{n} \right)_{h} = \left(b_{1}^{n} \right)_{h} - \left(d_{1}^{n} \right)_{h} \left\langle \bar{\mathbf{H}}_{h}^{n+1/2}, \nabla \phi_{h}^{n+1} \right\rangle - \left(d_{2}^{n} \right)_{h} \left[\left\langle \bar{g}_{h}^{n+1/2}, \phi_{h}^{n+1} \right\rangle + \left\langle \bar{h}_{h}^{n+1/2}, e_{h}^{n+1} \right\rangle \right], \, \left(\tilde{b}_{2}^{n} \right)_{h} = \left(b_{2}^{n} \right)_{h} - \left(d_{3}^{n} \right)_{h} \left[\left\langle \bar{g}_{h}^{n+1/2}, \phi_{h}^{n+1} \right\rangle + \left\langle \bar{h}_{h}^{n+1/2}, e_{h}^{n+1} \right\rangle \right]. \end{aligned}$$

Step 6. Update U_h^{n+1}, q_h^{n+1} via $U_h^{n+1} = U_h^n + \int_{\Omega} \bar{\mathbf{H}}_{\mathbf{h}}^{\mathbf{n}+1/2} \cdot \left(\nabla \phi_h^{n+1} - \nabla \phi_h^n\right) d\mathbf{r}, \ q_h^{n+1} = q_h^n + \int_{\Omega} \left(\bar{g}_h^{n+1/2} \left(\phi_h^{n+1} - \phi_h^n\right) + \bar{h}_h^{n+1/2} \left(e_h^{n+1} - e_h^n\right)\right) d\mathbf{r}.$

Step 7. Compute s_h^{n+1} , \mathbf{H}_h^{n+1} , De_h^{n+1} , g_h^{n+1} , h_h^{n+1} and T_h^{n+1} by their definitions in (5).

Note that we use V_h as both the trial and test function space in the finite element discretization.

Theorem 1. With periodic boundary conditions, the solution of the linear scheme exists uniquely for sufficiently small Δt , satisfies the discrete energy conservation law and preserves the entropy-production-rate preserving property:

$$\int_{\Omega} e_h^{n+1} d\mathbf{r} = \int_{\Omega} e_h^n d\mathbf{r}, \quad \frac{S_h^{n+1} - S_h^n}{\Delta t} \geqslant 0, \ n = 0, 1, 2, \dots,$$
 (15)

where $S_h^n = \int_{\Omega} \left[-\frac{\epsilon^2 k_0}{2} \left| \nabla \phi_h^n \right|^2 - \frac{C_0}{2} (\phi_h^n)^2 - \frac{C_1}{2} (e_h^n)^2 + A + B \right] d\mathbf{r} - \frac{1}{2} \left(U_h^n \right)^2 - \frac{1}{2} (q_h^n)^2.$

Proof. The solution existence and uniqueness for sufficiently small Δt is warranted by the solution existence and uniqueness of the equations in Step 2, 4, 5. Energy conservation follows from the following identity

$$\frac{\int_{\Omega} e_h^{n+1} d\mathbf{r} - \int_{\Omega} e_h^{n} d\mathbf{r}}{\Delta t} = \left\langle \frac{e_h^{n+1} - e_h^{n}}{\Delta t}, 1 \right\rangle = \int_{\Omega} -\nabla \cdot \left[\bar{D} e_h^{n+1/2} \nabla \left(-C_1 e_h^{n+1/2} - \bar{g}_h^{n+1/2} q_h^{n+1/2} \right) \right] d\mathbf{r}$$

$$= \int_{\partial \Omega} -\bar{D} e_h^{n+1/2} \mathbf{n} \cdot \nabla \left(-C_1 e_h^{n+1/2} - \bar{g}_h^{n+1/2} q_h^{n+1/2} \right) da = 0. \tag{16}$$

Then, we calculate the entropy increment:

$$\frac{S_h^{n+1} - S_h^n}{\Delta t} = \left\langle \left(\frac{\delta S}{\delta \phi} \right)_h^{n+1/2}, \phi_h^{n+1} - \phi_h^n \right\rangle + \left\langle -\nabla \cdot \left[\bar{D} e_h^{n+1/2} \nabla \left(\left(\frac{\delta S}{\delta e} \right)_h^{n+1/2} \right) \right], e_h^{n+1} - e_h^n \right\rangle \\
= \left\langle \bar{\tau}^{n+\frac{1}{2}} \delta_t \phi_h^n, \phi_h^{n+1} - \phi_h^n \right\rangle + \left\langle \delta_t e_h^n, e_h^{n+1} - e_h^n \right\rangle \ge 0.$$
(17)

It indicates the entropy increases and the rate of entropy production is preserved. \Box

Remark 1. For the physical boundary condition of the Neumann type, the results stand. In addition, high order temporal discretizations can be obtained using collocation techniques leading to implicit Runge–Kutta schemes. The spatial discretization, independent of the temporal discretization, can be done in any order with a proper treatment of boundary conditions in principle.

4. Numerical results

The fully discrete finite element scheme is implemented using deal-II with periodic boundary conditions in a rectangular domain $\Omega = [0, L_x] \times [0, L_y]$, and mesh sizes $h_x = L_x/N_x$ and $h_y = L_y/N_y$, where N_x and N_y are the number of meshes in each direction [6]. The Gaussian quadrature in each element is implemented using a 2nd order Legendre polynomial (a conforming C^0 element). In the mesh refinement test, we use $L_x = L_y = 0.5625$ and $N_x = N_y = 16$ and the initial value

$$\phi\left(\mathbf{x}, t = 0\right) = -0.5 tanh\left(\frac{\sqrt{0.018} - \sqrt{(x - 0.5L_x)^2 + (y - 0.5L_y)^2}}{\delta}\right) + 0.5,$$

$$e\left(\mathbf{x}, t = 0\right) = e_L\left(T_M\right) + C_L\left(0.5T_M - T_M\right) + \left(p\left(\phi\left(\mathbf{x}, t = 0\right)\right) - 1\right)\left(L_0 + L_1\left(0.5T_M - T_M\right)\right).$$
(18)

The parameter values used are $A = 100, B = 1, \theta_0 = \frac{\pi}{4}, \epsilon = 0.01, m = 4, \epsilon_4 = \frac{1}{m^2 - 1} = \frac{1}{15}, \tau = 3, e_L(T_M) = 0, k_0 = 1.0, C_L = 0.6, Du = 10^{-4}, L_1 = 0, L_0 = 0.5, T_M = 1, C_0 = 1, C_1 = 1, \delta = 0.1$. We observe the second order convergence in time, which is shown in Table 1.

Then we use the code to simulate a benchmark crystal growth example in a rectangular domain with $L_x = L_y = 4.5$ and $N_x = N_y = 256$. The initial values of ϕ , e and the parameters used are the same as given above except $\delta = 0.01$. In Fig. 1, the internal energy evolution and entropy evolution in time are plotted with time step $\Delta t = 0.004$ and m = 4. It demonstrates that the numerical scheme indeed guarantees energy conservation and entropy increase during time evolution.

Then we vary m = 4, 5, 6, 8 and use $\epsilon_4 = \frac{1}{m^2 - 1}$ in the simulations. Fig. 2 depicts snapshots of dentritic crystal growth patterns at four selected time slots, where we use blue to represent $\phi = 0$ (the solid) and

Table 1
Temporal mesh refinement test for the proposed scheme. Second order accuracy is established.

Coarse Δt	Fine Δt	L_2 Error of LS2	Order
0.5	0.25	0.0009733	1.8987
0.25	0.125	0.0002574	1.9447
0.125	0.0625	$6.578e{-05}$	1.9781
0.0625	0.03125	1.649e - 05	1.9972
0.03125	0.015625	$4.101e{-06}$	2.0052

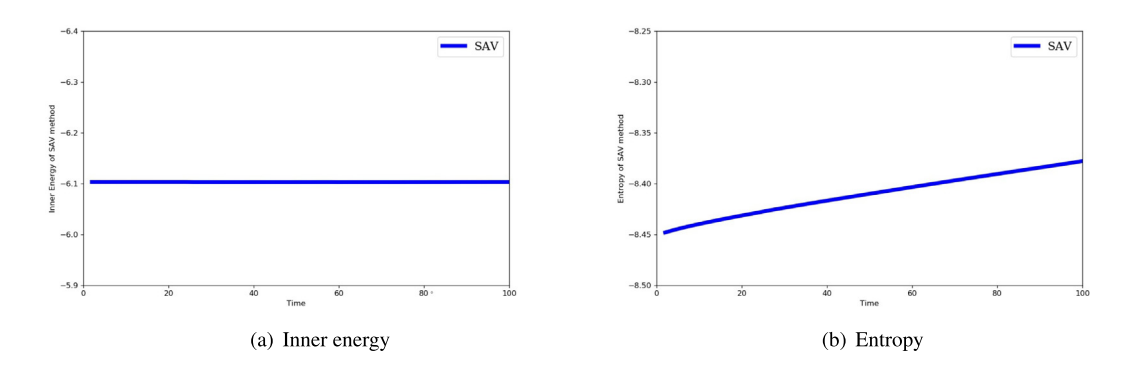


Fig. 1. Internal energy and entropy evolution of the model computed using SAV method with $\Delta t = 0.004$ and m = 4. They show that the energy is conserved and the entropy increases with time.

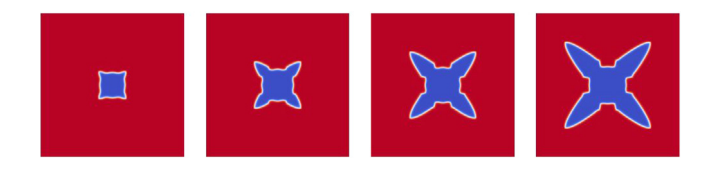


Fig. 2. Crystal growth of dendritic patterns with four folds. Snapshots of patterns at t=200,400,600,800, respectively, where $\Delta t=0.02$ and m=4.

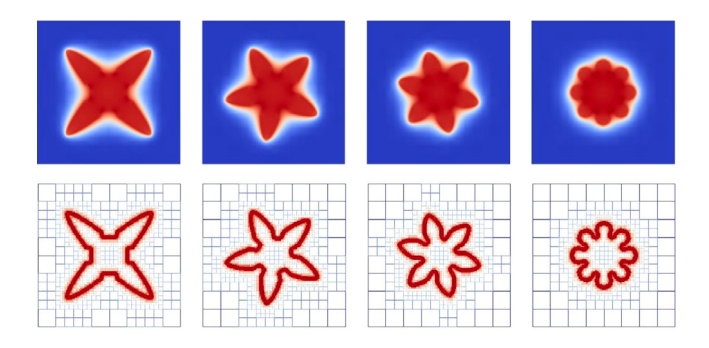


Fig. 3. Patterns of dendritic crystal growth with different folds at time t=800, where $\Delta t=0.02$ and m=4,5,6,8.

red $\phi=1$ (the liquid). We also color-code temperature T at time t=800 in Fig. 3, where blue represents T=0.5 and red represents T=1.0. We observe the release of latent heat during the process of solidification, the newly formed crystal region has higher temperature than the ambient liquid region. We note that all the simulations are computed using adaptive meshes in Deal.ii, allowing better resolution of the details near the interface.

References

- [1] O. Penrose, P.C. Fife, Thermodynamically consistent models of phase-field type for the kinetic of phase transitions, Physica D 43 (1) (1990) 44–62.
- [2] J. Li, J. Zhao, Q. Wang, Energy and entropy preserving numerical approximations of thermodynamically consistent crystal growth models, J. Comput. Phys. (2019).
- [3] J. Shen, J. Xu, J. Yang, The scalar auxiliary variable (SAV) approach for gradient flows, J. Comput. Phys. 353 (2018) 407–416.
- [4] S. Brenner, R. Scott, The Mathematical Theory of Finite Element Methods, Vol. 15, Springer Science & Business Media, 2007.
- [5] B. Gonzalez-Ferreiro, H. Gomez, I. Romero, A thermodynamically consistent numerical method for a phase field model of solidification, Commun. Nonlinear Sci. Numer. Simul. 19 (7) (2014) 2309–2323.
- [6] W. Bangerth, R. Hartmann, G. Kanschat, Deal. II—a general-purpose object-oriented finite element library, ACM Trans. Math. Softw. 33 (4) (2007) 24.